




## Fenofibrate ameliorates ocular surface inflammation in diabetic keratopathy

Hassan Mansoor<sup>a</sup>, Isabelle Xin Yu Lee<sup>b</sup>, Chang Liu<sup>b</sup>, Mingyi Yu<sup>b</sup>, Charmaine Jan Li Toh<sup>c</sup>, Victor Wei-Tsu Hsu<sup>b</sup>, Fengyi Liu<sup>d</sup>, Daqian Lu<sup>e</sup>, Thomas Chuen Lam<sup>e,f</sup>, Hong Chang Tan<sup>g</sup>, Lei Zhou<sup>h</sup>, Yu-Chi Liu<sup>b,i,j,k,l,\*</sup> 

<sup>a</sup> Al Shifa Trust Eye Hospital, Rawalpindi, Pakistan

<sup>b</sup> Tissue Engineering and Stem Cell Group, Singapore Eye Research Institute, Singapore

<sup>c</sup> Lee Kong Chian School of Medicine, Nanyang Technological University, Singapore

<sup>d</sup> University of Cambridge, Girton College, Cambridgeshire, United Kingdom

<sup>e</sup> Centre for Myopia Research, School of Optometry, The Hong Kong Polytechnic University, Hong Kong

<sup>f</sup> Centre for Eye and Vision Research (CEVR), 17W Hong Kong Science Park, Hong Kong

<sup>g</sup> Department of Endocrinology, Singapore General Hospital, Singapore

<sup>h</sup> School of Optometry, Department of Applied Biology and Chemical Technology, Research Centre for SHARP Vision (RCSV), The Hong Kong Polytechnic University, Hong Kong

<sup>i</sup> Cornea and Refractive Surgery Group, Singapore Eye Research Institute, Singapore

<sup>j</sup> Department of Cornea and External Eye Disease, Singapore National Eye Centre, Singapore

<sup>k</sup> Eye-Academic Clinical Program, Duke-National University Singapore Graduate Medical School, Singapore

<sup>l</sup> Department of Ophthalmology, National Taiwan University Hospital, Taiwan

### ARTICLE INFO

#### Keywords:

Ocular surface  
Cornea  
Inflammation  
Apoptosis  
Diabetes  
Fenofibrate

### ABSTRACT

**Purpose:** To investigate the efficacy of oral fenofibrate in the amelioration of ocular surface inflammation in diabetes mellitus (DM).

**Methods:** In this open-label interventional study, 41 participants with type 2 DM received oral fenofibrate for 30 days. Forty age-matched healthy controls were recruited. Ocular surface objective and subjective assessment, in-vivo confocal microscopy (IVCM) imaging and quantification for corneal dendritic cells (DCs), epithelium and neuromas were performed. Tear inflammatory markers and proteomics were analyzed with enzyme-linked immunosorbent assay (ELISA) and Data Independent Acquisition experiments before and after treatment.

**Results:** Oral fenofibrate treatment significantly improved tear film breakup time ( $p = 0.004$ ), corneal staining evaluated with National Eye Institute-Corneal Fluorescein Staining scores ( $p = 0.005$ ), and ocular surface symptoms assessed with the Ocular Surface Disease Index scores ( $p = 0.003$ ), in DM patients. On IVCM, fenofibrate significantly reduced mean DC area ( $p = 0.01$ ) and mean DC density ( $p = 0.02$ ), while increasing mean DC elongation ( $p = 0.004$ ) and length ( $p = 0.01$ ), suggesting less DC activities. Fenofibrate also significantly increased corneal epithelial cell density ( $p = 0.04$ ). 192 tear proteins were significantly altered after treatment. Fenofibrate significantly up-regulated the expression of anti-inflammatory interleukin-1 receptor antagonist, while significantly reduced the concentrations of pro-inflammatory and inflammatory proteins, including tumour necrosis factor  $\alpha$ , nuclear factor kappa B, complement 4 B, cytochrome B5 Type A, and cytochrome B5 Type B (all  $p < 0.05$ ) in tears, via regulation of tricarboxylic acid cycle, oxidative phosphorylation and liver X receptor/retinoid X receptor activation.

**Conclusion:** This first clinical trial demonstrated that oral fenofibrate ameliorates diabetic ocular surface inflammation, providing a novel therapeutic option for diabetic keratopathy.

\* Corresponding author. 11 Third Hospital Ave, 168751, Singapore.

E-mail address: [liuchi@gmail.com](mailto:liuchi@gmail.com) (Y.-C. Liu).

<https://doi.org/10.1016/j.jtos.2025.05.010>

Received 18 November 2024; Received in revised form 26 April 2025; Accepted 29 May 2025

Available online 30 May 2025

1542-0124/© 2025 The Authors. Published by Elsevier Inc. This is an open access article under the CC BY-NC-ND license (<http://creativecommons.org/licenses/by-nc-nd/4.0/>).

## 1. Introduction

Diabetes mellitus (DM) is a major public health issue, and it is anticipated that more than 342 million individuals globally will have diabetes by 2030 [1]. Existing evidence has suggested that chronic activation of pro-inflammatory pathways, involving both the innate and adaptive immune systems, contribute to the onset and progression of diabetes [1]. DM has been shown to have a negative impact on the ocular surface via a complex neurobiological and neuroinflammatory interplay [2]. Major negative impacts of DM on the ocular surface include an underdiagnosed corneal disorder known as diabetic keratopathy. This entity encapsulates different pathological conditions such as diabetic corneal neuropathy (DCN), impaired corneal epithelial wound healing and tear film, alterations in dendritic cells (DCs), and increased ocular surface inflammation [2–4]. Consequently, diabetic keratopathy (DK), an increasingly common ocular complication of DM, may ensue [5]. DK affects 47–64 % of diabetic patients during their clinical course and is frequently underdiagnosed [5].

DM-related ocular surface complications are caused by chronic hyperglycemia and its associated metabolic effects, such as the accumulation of advanced glycation end products (AGE), increased polyol pathway flux, reactive oxygen species (ROS) production, and activation of the protein kinase C (PKC) pathway [2]. The elevated AGE/RAGE (receptor for AGE) signaling triggers inflammatory and oxidative stress pathways, including the NF- $\kappa$ B (Nuclear factor kappa-light-chain-enhancer of activated B cells) signaling system, causing cell damage and death [6]. Activation of the NF- $\kappa$ B signaling system subsequently induces the release of tumour necrosis factor  $\alpha$  (TNF $\alpha$ ), interleukin-1 beta (IL-1 $\beta$ ), IL-6, and other pro-inflammatory cytokines [7], resulting in disease sequelae of corneal epithelial injury and neuronal destruction. Furthermore, AGE accumulation causes ROS-mediated apoptosis and hyperactivation of the NLRP3 (nucleotide-binding domain, leucine-rich-containing family, pyrin domain-containing-3) inflammasome, promoting pyroptosis and impairing corneal epithelial cell proliferation [8,9]. ROS and RAGE also trigger the phospholipase C/PKC/extracellular signal-regulated kinase activator protein 1 signaling pathway, exacerbating fibrogenesis by increasing transforming growth factor- $\beta$  expression [10]. These results highlight the pathogenic involvement of apoptosis, pyroptosis, and fibrogenesis in DK.

DCs in the cornea are bone marrow-derived antigen-presenting cells (APCs) that primarily trigger and exacerbate immunoinflammatory responses [4]. Several studies have found increased corneal DC density in DM [11,12], although a few reported the opposite [4,13,14]. The increase in DC density can be related to an inflammation-mediated cellular response, while the decrease in density can be attributed to apoptosis caused by prolonged hyperglycemia exposure [4]. Besides, patients with DM have a proportional increase in mature DCs (mDCs) and a proportional decrease in immature DCs (imDCs) [4,15]. Resident DCs in corneal epithelial wounds in DCN exacerbate the negative impact on the diabetic ocular surface [4,15,16]. One proposed mechanism is that inflammatory chemokines generated by the injured epithelium promote the recruitment of DCs to the corneal wound bed, adversely impacting the DC-epithelial cell interplay and worsening the inflammatory state [4,17,18]. As the interplay of inflammatory cytokines, corneal nerves and ocular surface integrity plays a major role in the pathogenesis of diabetic corneal surface, ocular surface inflammation may be an important target for developing therapeutics for diabetic ocular surface.

Peroxisome proliferator-activated receptors (PPARs) represent a family of nuclear hormone receptors. There are three subtypes (PPAR $\alpha$ , PPAR $\beta/\delta$ , and PPAR $\gamma$ ), with PPAR $\alpha$  being the most abundant in corneas [19]. Recent investigations in a rat alkali corneal injury model have shown that topical PPAR agonists reduced corneal inflammation and fibrosis while modulating corneal angiogenesis [20–24]. Of note, activation of all PPARs subtypes has been linked to suppressing the NF- $\kappa$ B pathway, which reduces corneal inflammation [25]. The promising

efficacy of PPAR agonists was mediated by reduced expression levels of IL-1, IL-6, IL-8, monocyte chemoattractant protein-1 (MCP-1), TNF $\alpha$ , transforming growth factor beta 1 and vascular endothelial growth factor-A (VEGF-A) [13–17]. Similarly, a PPAR $\beta/\delta$  agonist (GW501516) suppressed corneal inflammation by lowering mRNA expression of the aforementioned inflammatory cytokines [23].

Among PPARs, fenofibrate is a PPAR $\alpha$  agonist and an existing drug that modulates lipid metabolism and is commonly used to treat hyperlipidemia [26]. Emerging evidence indicates that fenofibrate has a protective effect on DM-related complications, such as diabetic retinopathy (DR), nephropathy, and cardiopathy [26]. The most recent data in the Fenofibrate Intervention and Event Lowering in Diabetes and The Action to Control Cardiovascular Risk in Diabetes Eye studies revealed that systemic fenofibrate slowed the progression of DR [27]. These therapeutic effects could be attributed to its potent anti-inflammatory properties, which could be achieved either directly through PPAR $\alpha$ -mediated suppression of inflammatory pathways or cytokines, such as NF- $\kappa$ B pathways and interleukins, or indirectly through normalizing tissue metabolic status, as deranged lipid metabolism leads to an inflammatory tissue environment and subsequently vascular complications [26].

Taken together, we postulated that fenofibrate has beneficial effects on the amelioration of ocular surface inflammation in DM. This clinical trial for the first time investigated the potential therapeutic effect of fenofibrate on the suppression of diabetic ocular surface inflammation and explored the mechanism of the treatment efficacy of fenofibrate, by assessing the clinical ocular surface, corneal DCs, epithelial cells and neuroma imaging, as well as tear inflammatory markers and proteomic profiles.

## 2. Methods

### 2.1. Study design and population

This was an open-label interventional study. Between October 2020 and September 2022, a total of 41 people with type 2 DM and 40 age-matched healthy controls were recruited from Singapore General Hospital and Singapore Eye Research Institute. The inclusion and exclusion criteria are detailed in Table 1. Healthy volunteers with no known systemic comorbidities, no long-term drugs usage, no corneal pathology, and no history of corneal or ocular surgery served as control subjects. The following data were collected: patients' age, gender, race, duration of DM, hemoglobin A1C (HbA1C), fasting glucose, as well as lipid profiles before and after fenofibrate treatment. The study was approved by SingHealth's institutional review board (ref no: 2020/2050 and R1678/1/2020), and it followed the Helsinki Declaration.

### 2.2. Fenofibrate treatment

Eligible subjects received oral fenofibrate for 30 days. The fenofibrate dosages were determined by the renal dosing prescription of the local drug regulatory authority. Subjects having a creatinine clearance time >60 mL/min received 300 mg/day of fenofibrate, whereas those with a value of 30–59 mL/min were given 100 mg/day of fenofibrate.

Ocular surface subjective and objective assessment, in-vivo confocal microscopy (IVCM) imaging for corneal DCs, epithelium and neuromas, tear analysis for inflammatory markers and proteomic profiles, were performed before and after fenofibrate treatment.

### 2.3. Ocular surface subjective and objective assessment

The subjective symptoms were assessed using the Ocular Surface Disease Index (OSDI) questionnaire [28]. The OSDI questionnaire contains 12 items covering three subscales: ocular symptoms, vision-related function, and environmental triggers. The study participants scored their responses for each item ranging from 0 to 4, where 0 represented

**Table 1**  
Inclusion and exclusion criteria of the clinical trial.

<b>Inclusion Criteria</b>
<ul style="list-style-type: none"> <li>• Aged <math>\geq 21</math> years</li> <li>• Type 2 DM, defined by</li> <li>• Fasting plasma glucose <math>&gt;7.0</math> mmol/L, or</li> <li>• Hyperglycemia symptoms with plasma glucose <math>&gt;11.1</math> mmol/L, or</li> <li>• 2-h plasma glucose <math>&gt;11.1</math> mmol/L after a 75-g oral glucose load</li> <li>• Known type 2 DM duration of at least 3 months</li> <li>• Mild to moderate diabetic nephropathy, characterized by a diminished creatinine clearance time (CCT) (between 30 and 60 mL/min) and/or albuminuria</li> <li>• HbA1C of <math>&lt;9\%</math> (<math>&lt;75</math> mmol/mol) within 3 months before the enrollment</li> <li>• No changes in the lipid- and glucose-lowering medication dosages in the previous 3 months</li> </ul>
<b>Exclusion Criteria</b>
<ul style="list-style-type: none"> <li>• Type 1 DM</li> <li>• Recent 3 months history of instilling eye drops that may affect the analysis of ocular surface inflammatory markers, such as topical or oral steroids, non-steroidal anti-inflammatory drugs, and immunosuppressants such as cyclosporin</li> <li>• History of laser refractive surgical procedure and/or chronic contact lens usage (<math>&gt;6</math> months)</li> <li>• Concurrent ocular surface disease, such as active keratitis, ocular rosacea, and corneal scars or opacity</li> <li>• Concurrent usage of medications that would interfere with the fenofibrate treatment (e.g., systemic steroids, bile acid sequestrants, tacrolimus etc)</li> <li>• Severe renal impairment characterized by CCT <math>&lt;30</math> mL/min or renal replacement therapy</li> </ul>

“none of the time” and 4 represented “all of the time.” Subsequently, an overall OSDI score was calculated using the formula; OSDI Score = (Sum of responses in each subscale)  $\times$  25/Total number of questions answered [29]. Following the OSDI score evaluation, the objective assessments were conducted in the following order: Tear Breakup Time (TBUT), Ocular Surface and Corneal Staining, Schirmer’s test, and finally, In Vivo Confocal Microscopy (IVCM) imaging.

The tear breakup time (TBUT) was recorded by placing a sterile fluorescein strip into the inferior fornix and measuring the time interval (seconds) between opening the eyes and the first dry spot that appeared on the corneal surface [30]. The TBUT was measured three times, with the mean value recorded for analysis. Fluorescein sodium staining was performed to assess the integrity of the ocular surface using the pre-sterilized 1 mg fluorescein sodium ophthalmic strips (BioGlo™, Bernell Corporation, IN, USA). The Oxford grading scale that ranges from 0 (no staining) to 5 (severe staining) was used to grade ocular surface staining by placing a drop of sterile saline on a pre-sterilized fluorescein strip [31–33]. Likewise, the National Eye Institute-Corneal Fluorescein Staining (NEI-CFS) score was used to evaluate the level of corneal punctate staining by using the pre-sterilized fluorescein strips. Subsequently, the cornea was divided into five areas by a five-region grid that was overlaid onto the cornea, with the central region representing one-third of the corneal diameter and the width of the surrounding quadrants also representing one-third of the corneal diameter. The dot count was employed to grade the level of punctate staining in each corneal region (Grade 0: 0 dots; Grade 1: 1 to 15 dots; Grade 2: 16 to 30 dots; Grade 3:  $>30$  dots) [34]. Thereafter, each section of the cornea received a NEI-CFS score ranging from 0 (absent) to 3 (severe), with a maximum possible score of 15, depending on the size, amount and confluence of the punctate lesions [34]. For Schirmer’s test, the Schirmer’s strips were placed on the inferior temporal half of the lower lid border in both eyes without topical anesthesia, and the wet length after 5 min was measured. The strips were then immediately transferred to the laboratory and stored at  $-80^\circ\text{C}$  until the day of analysis.

#### 2.4. In-vivo confocal microscopy (IVCM) for corneal dendritic cells, epithelium and neuromas

IVCM scans (HRT3 with Rostock Corneal Module; Heidelberg Engineering, Heidelberg, Germany) were performed under topical anesthesia by an experienced ophthalmologist (C.L) masked to the study groups with the standardized protocol we previously described [35]. A carbomer gel was applied onto and over the objective lens as an immersion fluid, and a Tomo-cap was attached to cover the lens. In brief, the central cornea was scanned first. To stabilise the scanning view, the patient was instructed to fixate on a light source in various directions with the contralateral eye. Subsequently, the superior, inferior, nasal,

and temporal corneal regions were scanned, each approximately 3 mm away from the corneal apex, covering a  $400 \times 400 \mu\text{m}^2$  field of view. The cornea was scanned from the epithelium to the endothelium.

Corneal DCs were defined as small and bright dendriform cells [4]. Good-quality epithelial images were defined as images with good clarity of the epithelial border and  $>85\%$  area covered by epithelial cells within the IVCM micrograph [36]. Five best-quality images from each area, totaling 25 images for DCs and 25 images for epithelium, respectively, were selected for further analysis. The AIconfocal Rapid Image Evaluation System software (ARIES; ADCIS, Saint-Contest, Basse--Normandie, France) was used to quantify the following DCs parameters: density (cells/ $\text{mm}^2$ ); area ( $\mu\text{m}^2$ ); average length ( $\mu\text{m}$ ) (the average width of all DCs analyzed by software); elongation ( $\mu\text{m}$ ) (the absolute value of the major(x)-minor(y) axis difference divided by the sum of the major and minor axis ( $x-y/x+y$ )). Analyzed corneal epithelial parameters included cell density (cells/ $\text{mm}^2$ ); cell size ( $\mu\text{m}^2$ ); cell circularity. Cell circularity represents how closely the shape of cells approaches that of a circle. A circularity value of 1.0 indicates an ideal circle, and the value decreases with increasing deviation from a circle.

The corneal neuromas were defined as microscopic, irregularly shaped enlargements of terminal nerve endings. All images including corneal neuromas were selected, and the same corneal neuroma was only selected once. The images were manually quantified for the neuroma area ( $\mu\text{m}^2$ ), average length ( $\mu\text{m}$ ) and perimeter ( $\mu\text{m}$ ) using Image J (National Institute of Health, Bethesda, MD).

Both eyes of the participants were included for IVCM imaging and the quantitative analysis. Each image was independently selected and evaluated for corneal DCs, epithelium and neuromas by an independent, experienced, and masked ophthalmologist (M.Y.Y.).

#### 2.5. Analysis for tear inflammatory markers

Tear inflammatory markers in all tear samples collected from the Schirmer tests were analyzed using the enzyme-linked immunosorbent assay (ELISA) [37]. Schirmer strips with tear fluid samples were minced and submerged in 200  $\mu\text{L}$  elution buffer consisting of 0.55M NaCl, 0.33 % Tween 20, 0.55 % Bovine Serum Albumin, and protease inhibitor. Samples were subjected to agitation and sonication at 20 % amplitude for 20 s before incubating at 450 rpm for 17 h at  $4^\circ\text{C}$ . The eluted tears were subsequently centrifuged and clear supernatant were collected [38]. ELISA was performed according to manufacturer’s protocol (IL-6 and TNF $\alpha$ ; R&D Biosystem; IL-1 $\beta$  and NF $\kappa\text{B}$ ; Abcam). The eluted tear samples were diluted (Dilution factor: 1.5x) to a volume 33.3  $\mu\text{L}$  per well with either sample, calibrator diluent provided in the ELISA kit or water. Background optical density reading was set at 540 nm. A microplate reader (Tecan Trading AG; Männedorf, Switzerland) was used to read the optical density at 450 nm, and the concentrations of the

neuromediators were subsequently interpolated from a standard curve.

## 2.6. Tear quantitative proteomic analysis

A previously described technique was used [39,40]. After cutting the schirmer's strips from the Schirmer's tests into small pieces, 100  $\mu$ L of lysis buffer was added and mixed in a ThermoMixer for 1.5 h at 20 °C. The Bio-Rad DC Protein assay determined the total protein content. Using the reagents from the EasyPep Mini Sample Prep Kits (Thermo Fisher Scientific, San Jose, CA), 100  $\mu$ g of eluted tear proteins were reduced, alkylated, digested with trypsin, and then desalted. A fluorometric peptide quantification kit was used to calculate the total peptide quantity. The peptide sample was then resuspended in 2 % acetonitrile with 0.1 % formic acid with iRT (1:10 ratio; Biognosys). An EASY-nLC 1200 system connected to an Orbitrap Exploris 480 mass spectrometer by an EASY-Spray source was used to analyse all peptide samples (1  $\mu$ g of total peptides per sample). An Acclaim PepMap 100C18 precolumn and a PepMap RSLC C18 analytical column were used for liquid chromatographic separation. A 60-min gradient comprising of 0.1 % formic acid as buffer A, and 80 % acetonitrile in 0.1 % formic acid as buffer B, separated the peptides. Data independent acquisition (DIA) experiments were used to perform quantitative proteomic analysis. A total of nineteen 45.7 Da windows were used, with a 3 Da overlap. DIA data were analyzed in Spectronaut 15 (Biognosys) using the library-free directDIA protocol. All statistical analyses used raw abundance data that was median normalised and log transformed. A fold change (FC)  $\geq 1.5$  and  $\text{FC} \leq -1.5$  with an adjusted P value of  $<0.05$  were considered significant. Ingenuity Pathways Analysis (IPA) was used to identify enriched pathways [41]. Custom scripts in R (64-bit version 4.1.1) was used to perform the downstream data analysis and data visualization [39].

## 2.7. Statistical analysis

The required sample size was calculated based on the data of the primary outcome, which is DC density, from the pilot 6 DM patients. The mean DC density was  $0.022 \pm 0.002$  (cells/mm<sup>2</sup>) and  $0.021 \pm 0.002$  (cells/mm<sup>2</sup>) before and after fenofibrate treatment, respectively. Therefore, a sample size of 34 patients with a power of  $\geq 80\%$  and a level of significance of 5 % was sufficient to detect the difference before and after fenofibrate treatment. We therefore recruited 41 DM patients, anticipating a 15 % loss to follow-up. The normality of data distribution was assessed with a Kolmogorov-Smirnov test. To account for the correlation of the paired time points and both eyes, linear mixed models were used for normally distributed data, and generalized linear mixed models were conducted for non-normally distributed data [42], to analyse the data before and after treatment, as well as the data of the control subjects and the DM group (pre-treatment). All data are presented as mean  $\pm$  SD. Stata 17 (StataCorp, College Station, TX) was used for the statistical analysis, and  $p < 0.05$  was considered significant.

## 3. Results

### 3.1. Demographic and clinical characteristics of DM patients with fenofibrate treatment

Of the 41 DM patients, 28 (78 %) and 8 (22 %) patients were prescribed oral fenofibrate at doses of 100 mg/day and 300 mg/day, respectively. The mean age in the DM group was  $59.7 \pm 11.7$  years, while in the control group it was  $63.7 \pm 7.1$  years ( $p = 0.47$ ). In the DM group, the majority of the patients were men (72 %) and Chinese (83 %). The average DM duration was  $18.7 \pm 9.8$  years. The mean HbA1c and fasting glucose levels in the DM group were  $7.7 \pm 1.1\%$  and  $7.4 \pm 1.9$  mmol/L, respectively. DM patients had significantly higher HbA1c and LDL levels than controls (95 % Confidence Interval (CI) of mean difference 1.08–2.11 %;  $p < 0.001$ ) and (95 % CI of mean difference 0.67–2.12 mmol/L;  $p < 0.001$ ), respectively. Following fenofibrate

treatment, blood triglyceride levels reduced from  $1.6 \pm 0.9$  to  $1.4 \pm 0.8$  mmol/L (95 % CI of mean difference 0.05–0.64 mmol/L;  $p = 0.002$ ), indicating good compliance of fenofibrate treatment. The DM patients did not experience any serious fenofibrate-related adverse effects [43] or discontinued the treatment due to intolerance. The other baseline parameters were comparable between the DM cohort and the control group (all  $p > 0.05$ ).

### 3.2. Fenofibrate significantly reduced corneal dendritic cell infiltrate

The mean corneal DC density was significantly reduced from  $0.022 \pm 0.002$  cells/mm<sup>2</sup> to  $0.021 \pm 0.002$  cells/mm<sup>2</sup> after treatment (95 % CI of mean difference 0.0001–0.0019 cells/mm<sup>2</sup>;  $p = 0.02$ ) (Fig. 1A–D). Before treatment, the mean DC area in the DM group was larger than that in the control group ( $47.9 \pm 5.8 \mu\text{m}^2$  versus  $45.9 \pm 5.7 \mu\text{m}^2$ ) (95 % CI of mean difference 0.4–4.8  $\mu\text{m}^2$ ;  $p = 0.04$ ). After treatment, it was significantly reduced to  $45.4 \pm 4.4 \mu\text{m}^2$  (95 % CI of mean difference  $-0.76$  to  $-4.36 \mu\text{m}^2$ ;  $p = 0.01$ ) (Fig. 1E). Furthermore, both DC elongation (Fig. 1F) and DC length (Fig. 1G) significantly increased after fenofibrate treatment (from  $0.60 \pm 0.20 \mu\text{m}$  to  $0.62 \pm 0.30 \mu\text{m}$ ) (95 % CI of mean difference 0.06–0.21  $\mu\text{m}$ ;  $p = 0.002$ ; (from  $10.63 \pm 1.70 \mu\text{m}$  to  $11.12 \pm 1.96 \mu\text{m}$ ) (95 % CI of mean difference 0.14–0.84  $\mu\text{m}$ ;  $p = 0.01$ ) respectively, indicating that fenofibrate treatment shifts the DC equilibrium towards a more immature phenotype.

### 3.3. Fenofibrate significantly improved corneal epithelial cell density (CECD)

Compared to normal subjects, DM patients presented with a significantly lower CECD ( $8759 \pm 36$  cells/mm<sup>2</sup> versus  $7698 \pm 48$  cells/mm<sup>2</sup>) (95 % CI of mean difference  $-818.3$  to  $-432.5$  cells/mm<sup>2</sup>;  $p = 0.003$ ) (Fig. 2A–D), significantly worse epithelial cell circularity ( $0.71 \pm 0.02$  versus  $0.72 \pm 0.01$ ) (95 % CI of mean difference 0.006–0.012;  $p = 0.03$ ) (Fig. 2E), and significantly larger epithelial cell size ( $128.2 \pm 5.6 \mu\text{m}^2$  versus  $133.5 \pm 20.8 \mu\text{m}^2$ ) (95 % CI of mean difference 1.2–9.7  $\mu\text{m}^2$ ;  $p = 0.03$ ) (Fig. 2F). These indicate that diabetic corneal epithelial cells were less compact and more swollen. After fenofibrate treatment, CECD increased significantly to  $8164 \pm 17$  cells/mm<sup>2</sup> (95 % CI of mean difference 252.5–713.0 cells/mm<sup>2</sup>;  $p = 0.01$ ) in DM patients (Fig. 2D).

### 3.4. Corneal neuromas after fenofibrate treatment

We found that corneal neuromas were present in 61.8 % of diabetic eyes and 31.2 % in healthy subjects (Chi-square test:  $p < 0.001$ ). Compared to controls, diabetic eyes had significantly larger neuroma area ( $10.1 \pm 1.6 \mu\text{m}^2$  versus  $645.1 \pm 452.3 \mu\text{m}^2$ ) (95 % CI of mean difference 633.6–641.7  $\mu\text{m}^2$ ;  $p < 0.001$ ), neuroma length ( $15.8 \pm 3.4 \mu\text{m}$  versus  $161.1 \pm 115.1 \mu\text{m}$ ) (95 % CI of mean difference 144.1–146.2  $\mu\text{m}$ ;  $p < 0.001$ ), and perimeter ( $2.5 \pm 0.9 \mu\text{m}$  versus  $53.1 \pm 25.1 \mu\text{m}$ ) (95 % CI of mean difference 50.1–52.2  $\mu\text{m}$ ;  $p < 0.001$ ). These neuroma parameters were not significantly changed after treatment (post-treatment neuroma area:  $617.1 \pm 375.6 \mu\text{m}^2$ ,  $p = 0.72$ ; post-treatment neuroma length:  $160.6 \pm 123.2 \mu\text{m}$ ,  $p = 0.98$ , post-treatment neuroma perimeter  $51.9 \pm 26.2 \mu\text{m}$ ,  $p = 0.85$ ).

### 3.5. Fenofibrate significantly improved the corneal staining, TBUT and OSDI

The NEI-CFS score, TBUT and OSDI score were significantly worse in the DM group than in the control group; NEI-CFS score:  $1.67 \pm 1.38$  versus  $0.72 \pm 0.69$  (95 % CI of mean difference 0.11–0.82;  $p = 0.04$ ), TBUT:  $5.1 \pm 2.4$  s versus  $8.5 \pm 3.6$  s (95 % CI of mean difference  $-2.1$  to  $-1.0$  s;  $p = 0.002$ ), OSDI score:  $4.7 \pm 3.8$  points versus  $1.0 \pm 1.9$  points (95 % CI of mean difference 1.8–3.6 points;  $p = 0.002$ ). After fenofibrate treatment, the NEI-CFS score, TBUT and OSDI score significantly improved to  $1.23 \pm 1.11$  (95 % CI of mean difference  $-0.73$  to  $-0.14$ ;  $p$



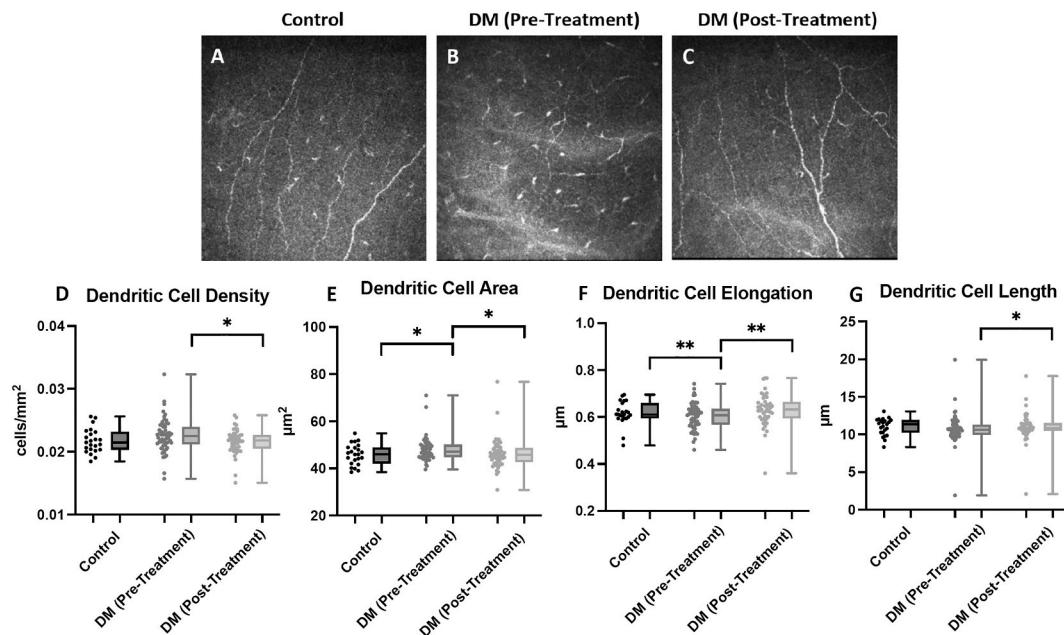


**Fig. 1.** Effects of fenofibrate treatment on corneal dendritic cell (DC) parameters. Representative IVCN images of corneal DCs in (A) Control (B) DM (Pre-Treatment) and (C) DM (Post-Treatment) groups. (D–G) The box and whisker plots showing the DC density, DC area, DC elongation and DC length in the Control, DM (Pre-Treatment) and DM (Post-Treatment) groups, respectively. \* represents  $p < 0.05$ , \*\* represents  $p < 0.01$ .

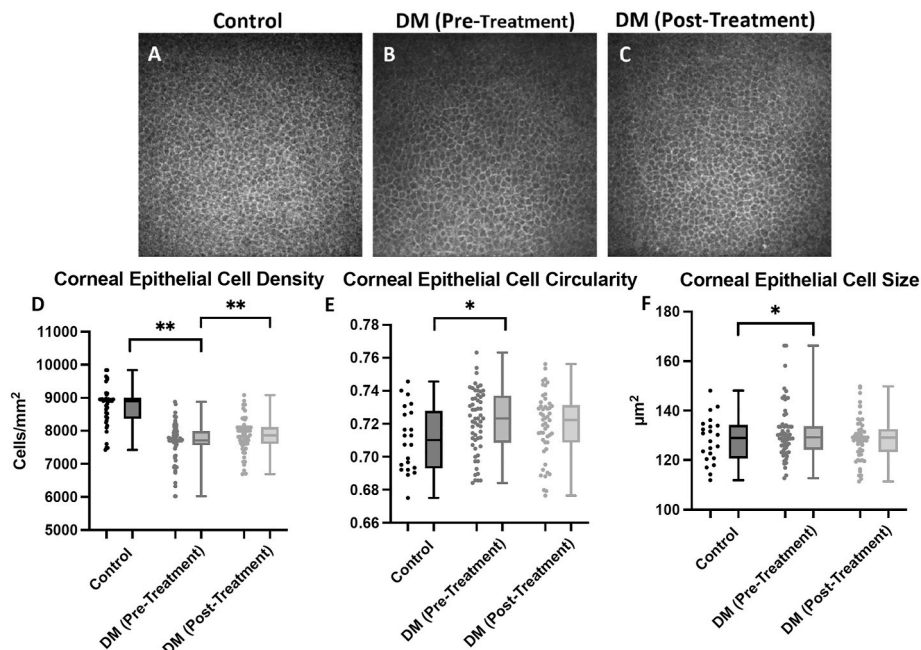


**Fig. 2.** Effects of fenofibrate treatment on corneal epithelial cell parameters. Representative IVCN images of corneal epithelial cells in (A) Control (B) DM (Pre-Treatment) and (C) DM (Post-Treatment) groups. (D–F) The box and whisker plots showing the epithelial cells' density, circularity and size in the Control, DM (Pre-Treatment) and DM (Post-Treatment) groups, respectively. \* represents  $p < 0.05$ , \*\* represents  $p < 0.01$ .

= 0.004),  $6.6 \pm 2.1$  s (95 % CI of mean difference 0.49–1.50 s;  $p = 0.005$ ), and  $1.8 \pm 2.7$  points (95 % CI of mean difference –2.49 to –1.71 points;  $p = 0.005$ ), respectively (Fig. 3A–C). The Oxford grading score and Schirmer's test values did not differ significantly between the control and DM groups, as well as between before and after fenofibrate treatment (Fig. 3D and E).

### 3.6. Fenofibrate significantly reduced tear $TNF\alpha$ and $NF-\kappa B$ levels

The level of the tear inflammatory cytokines, including  $TNF\alpha$ ,  $NF-\kappa B$ , IL-1 and IL-6 were significantly higher in the DM group compared to the control group;  $TNF\alpha$ :  $1.92 \pm 0.73$  pg/ml versus  $1.55 \pm 1.08$  pg/ml (95 % CI of mean difference 0.01–0.29 pg/ml;  $p = 0.03$ ),  $NF-\kappa B$  expression:  $848.7 \pm 852.6$  ng/ml versus  $594.1 \pm 394.5$  ng/ml (95 % CI of mean difference 28.1–472.1 ng/ml;  $p = 0.03$ ), IL-1:  $1.64 \pm 2.49$  pg/ml versus  $0.93 \pm 1.35$  pg/ml (95 % CI of mean difference 0.14–0.38 pg/ml;  $p =$

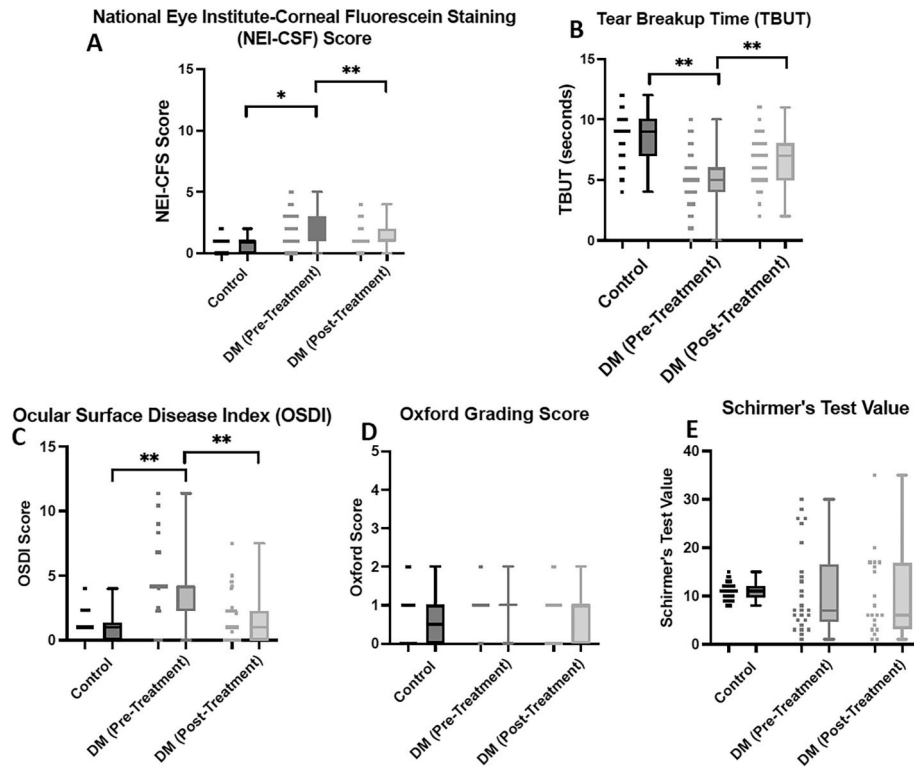


**Fig. 3.** Subjective and objective ocular surface assessment before and after fenofibrate treatment. The box and whisker plots show that, while the (A) NEI-CFS score (B) TBUT, and (C) OSDI score improved significantly in the DM group after fenofibrate treatment, the (D) Oxford grading score and (E) Schirmer's test values did not differ before and after fenofibrate treatment. Each dot on the y-axis of the box and whisker plot represents a data point from an individual study participant. \* represents  $p < 0.05$ , \*\* represents  $p < 0.01$ .

0.006), IL-6:  $2.65 \pm 3.53$  pg/ml versus  $0.98 \pm 1.12$  pg/ml (95 % CI of mean difference 1.2–2.2 pg/ml;  $p = 0.005$ ) (Fig. 4A–D). The tear TNF $\alpha$  and NF- $\kappa$ B levels were significantly reduced to  $1.74 \pm 0.60$  pg/ml (95 % CI of mean difference  $-0.34$  to  $-0.01$  pg/ml;  $p = 0.04$ ) and  $598.3 \pm 481.5$  ng/ml (95 % CI of mean difference  $-470.51$  to  $-30.26$  ng/ml;  $p = 0.02$ ), respectively, after fenofibrate treatment.

### 3.7. Fenofibrate significantly up-regulated anti-inflammatory and down-regulated pro-inflammatory tear protein expression

The IPA showed that amongst the 1315 proteins measured, 68 were up-regulated and 124 down-regulated following treatment with fenofibrate (Fig. 5A). Fenofibrate treatment significantly increased the expression of interleukin-1 receptor antagonist (IL-1RN) ( $\log_2FC = 1.5$ ;

$p = 0.03$ ) (Fig. 5B) but significantly reduced the expression of the pro-inflammatory proteins, complement 4 B (C4B) ( $\log_2FC = 0.73$ ;  $p = 0.01$ ), cytochrome B5 Type A (CYB5A) ( $\log_2FC = 0.81$ ;  $p = 0.03$ ) and cytochrome B5 Type B (CYB5B) ( $\log_2FC = 0.80$ ;  $p = 0.04$ ) in tears of DM patients (Fig. 5C–E). Pathway analysis showed that proteins altered following fenofibrate treatment are associated with pathways related to: 1) Integrin signaling, 2) Oxidative phosphorylation, 3) Liver X receptor/Retinoid X receptor (LXR/RXR) activation 4), Actin cytoskeleton signaling, and 5) Tricarboxylic acid [44] cycle (Fig. 5F).

## 4. Discussion

DM is characterized by chronic low-grade inflammation [15]. Chronic hyperglycemia produces oxidative stress, activates coagulation

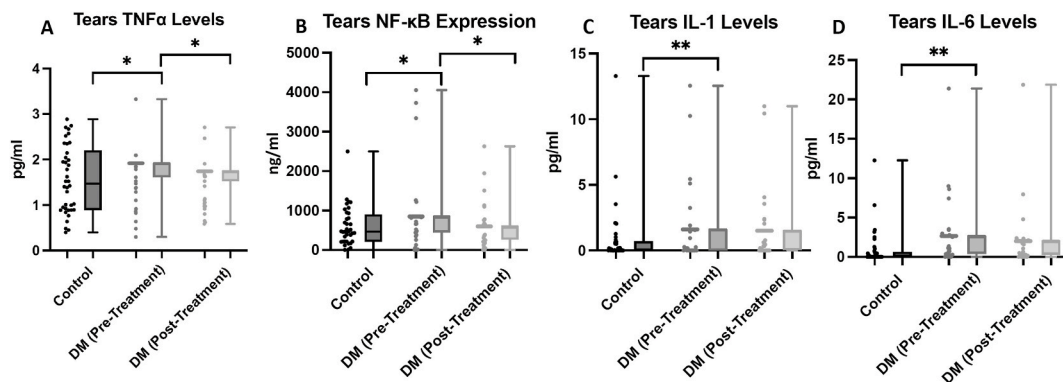


**Fig. 4.** Effects of fenofibrate treatment on tear inflammatory cytokines. The box and whisker plots showing the tear inflammatory cytokines (A) TNF $\alpha$ , (B) NF- $\kappa$ B, (C) IL-1 and (D) IL-6 in the Control, DM (Pre-Treatment) and DM (Post-Treatment) groups, respectively. After fenofibrate treatment, the concentration of TNF $\alpha$  and NF- $\kappa$ B in tears were significantly reduced in the DM group. \* represents  $p < 0.05$ , \*\* represents  $p < 0.01$ .

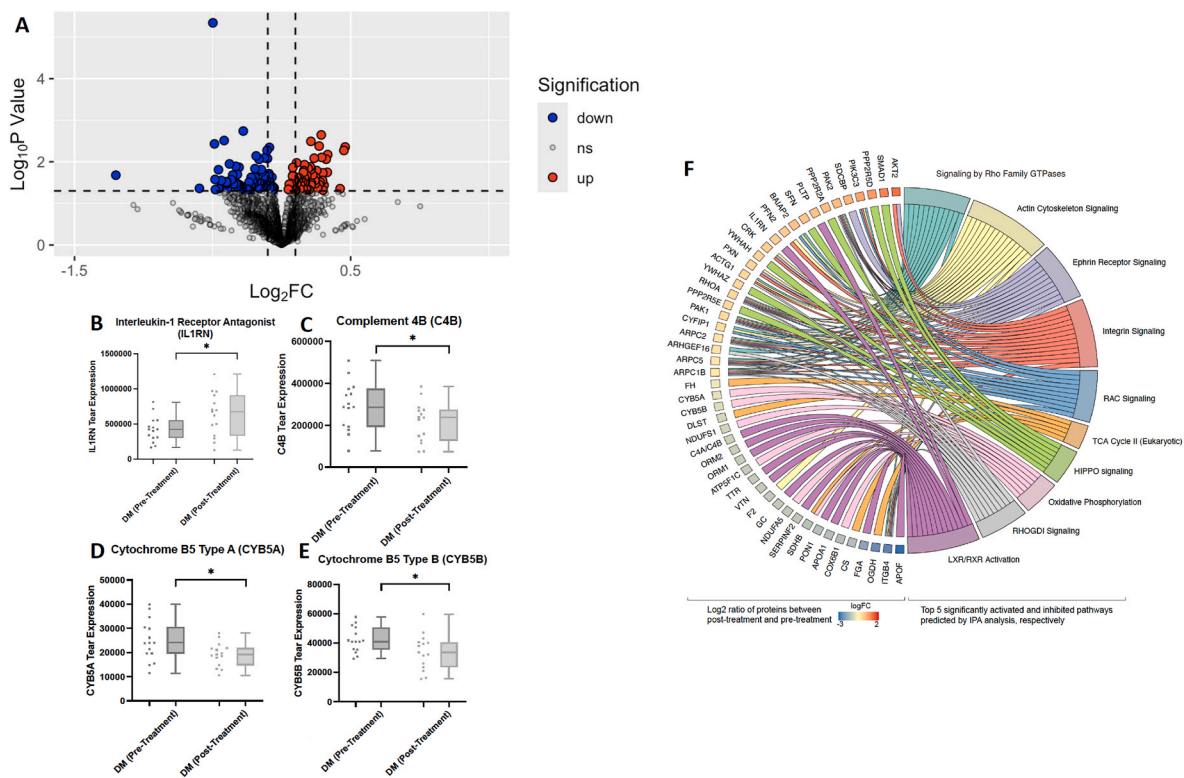


**Fig. 5.** Tear proteomic analysis on the effects of fenofibrate treatment on inflammatory tear protein expression. (A) Volcano plots presenting the FC of the tear proteins comparing DM patients with controls. Significantly up-regulated and down-regulated proteins ( $FC \geq 1.5$  and  $FC \leq -1.5$  with an adjusted P value of  $<0.05$ ) are shown in red and blue, respectively. The box and whisker plots demonstrate a significantly up-regulated (B) tear IL1-RN levels, and a significantly down-regulated (C) C4B, (D) CYB5A, and (E) CYB5B levels after fenofibrate treatment. \* represents  $p < 0.05$ . (F) Chord plot demonstrates the expressed biological pathways associated with the top 25 significantly up-regulated and top 25 significantly down-regulated proteins. (For interpretation of the references to colour in this figure legend, the reader is referred to the Web version of this article.)

factors, and enhances the expression of adhesion molecules, matrix metalloproteinases, and cytokines, resulting in a pro-inflammatory state. The pro-inflammatory microenvironment on the ocular surface triggers apoptosis, pyroptosis and altered fibrogenesis, thus leading to corneal epithelial and neuronal damage [8–10]. As a result, DK, an increasingly common but underdiagnosed ocular complication of DM, may develop [2,45–47]. Scientific efforts are underway to explore effective treatment options for reducing ocular surface inflammation in diabetic corneas and thereby the burden of its associated keratopathy. Our study is the first clinical trial to demonstrate that oral fenofibrate reduces DM-associated ocular surface inflammation. We demonstrated that fenofibrate significantly reduced corneal DCs overexpression, increased CECD, improved TBUT, ameliorated corneal staining and subjective ocular surface symptoms. On the molecular level, fenofibrate significantly suppressed tear  $TNF\alpha$  and  $NF-\kappa B$  levels. Quantitative proteomic analyses revealed that fenofibrate significantly increased tear IL1-RN and decreased C4B, CYB5A and CYB5B concentrations via regulation of TCA cycle, oxidative phosphorylation and liver X receptor/retinoid X receptor activation.

On IVCN evaluation, fenofibrate significantly increased mean DC elongation and length, along with a decrease in mean DC density and area. These suggest that fenofibrate treatment shifts the DC morphology equilibrium towards a more imDCs phenotype, indicating a reduction in ocular surface inflammation [4]. Aggarwal et al. presented that in patients with dry eye disease, the corneal staining is associated with DC size, DC density, and number of DCs, while conjunctival staining is associated with DC density [48]. This is consistent with our findings that showed that DC overexpression resulted in significantly worse NEI-CFS score, TBUT, and OSDI score in DM patients, which markedly improved after fenofibrate treatment. Furthermore, DM patients had significantly

lower CECD, worse epithelial cell circularity, and larger epithelial cell size than healthy individuals, indicating that diabetic corneal epithelial cells were less compact and more swollen. Our group previously demonstrated strong  $PPAR\alpha$  immunosignals in the epithelial layer of non-diabetic mice corneas, while diabetic mice corneal epithelial layer exhibited decreased  $PPAR\alpha$  expression [49]. This downregulation of  $PPAR\alpha$  expression in diabetic human corneas might result in reduced mitochondrial oxidative phosphorylation, a primary source of ATP production for corneal epithelial cell turnover, leading to impaired corneal epithelial morphology [50].  $PPAR\alpha$  knockout mice also demonstrated reduced mitochondrial metabolism and worse corneal epithelial healing compared to wild-type mice, suggesting that  $PPAR\alpha$  regulates epithelial wound healing [50]. Another possible explanation is the structural anomalies caused by the accumulation of AGE, which reduces the adhesion in corneal epithelium, resulting in morphological changes in DM patients [51,52]. Furthermore, corneal denervation in diabetic corneas affects the blink reflex and corneal epithelial cell survival due to reduced trophic support, potentially impairing corneal epithelial homeostasis [2,50]. The morphology of corneal epithelial cells improved after fenofibrate treatment, evidenced by the reduced cell size and edema, and significantly increased CECD. This could be attributed to an increase in neurotrophic factors following fenofibrate-induced corneal nerve regeneration, as demonstrated in our previous studies [49,53].

Clinically, fenofibrate treatment resulted in significant improvements in NEI-CFS scores, TBUT and OSDI scores in DM patients, indicating that fenofibrate promotes ocular surface homeostasis. Recent investigations in animal models have shown that activation of all  $PPARs$  subtypes promotes corneal epithelial homeostasis and wound healing through various pathways [20–24]. A 0.05 % solution of GW50516, a

PPAR $\delta$  agonist, was shown to promote corneal epithelial healing in a rat corneal alkali burn by enhancing the proliferative capability of epithelial cells [25]. Another study found that applying a PPAR $\delta$  agonist topically to a rat alkali-injury model reduced corneal epithelial cell death [54]. Similarly, a combination of PPAR $\alpha$  and PPAR $\gamma$  agonists promoted corneal epithelial wound repair in a rat alkali-injury model [22]. Another explanation for improved NEI-CFS scores, TBUT and OSDI scores could be fenofibrate-induced corneal nerve regeneration and improved corneal nerve metrics, as demonstrated in our published study [53]. In our published clinical trial, we demonstrated that 1-month oral fenofibrate treatment enhanced corneal nerve regeneration through upregulation of neurotrophic, lipid modulatory, anti-inflammatory, and anticoagulant pathways [53]. Based on these positive findings, we further formulated fenofibrate into topical eye drops and presented similar beneficial effects of topical fenofibrate in stimulating corneal nerve regeneration in a diabetic mice model [49]. The corneal innervation maintains a healthy ocular surface by providing trophic support [2]. The observed subjective and objective improvement in diabetic ocular surface can be attributed to the anti-inflammatory effects of fenofibrate as identified in this study or the increase of neurotrophin signaling and neurotrophic factors following fenofibrate-mediated corneal nerve regeneration as established in our prior investigations [49,53], or both. The Oxford grading score did not differ significantly before and after fenofibrate treatment. This could be because the Oxford grading scale (1–5) is cruder than the NEI-CFS scale (0–15).

Recent animal studies have demonstrated the anti-inflammatory properties of fenofibrate in non-corneal tissues [55,56]. In the peripheral nerves of diabetic mice, oral fenofibrate reduced neuro-inflammation and promoted axon regeneration by activating PPAR $\alpha$  receptors [55,56]. Furthermore, oral fenofibrate effectively reduced inflammatory mediators such as intercellular adhesion molecule-1, MCP-1, TNF $\alpha$ , and VEGF-A in the retinas of hyperglycemic mice [57]. Similarly, in this clinical trial, we found that fenofibrate significantly reduced tear TNF $\alpha$  and NF- $\kappa$ B levels. TNF $\alpha$  is a proinflammatory cytokine and a potent inducer of apoptosis, produced by macrophages and other innate immunity cells, which play a crucial role in activating the adaptive immunity through chemotactic processes [58,59]. Previous studies have shown that DM patients had higher circulating levels of TNF $\alpha$  [60–62], with TNF $\alpha$  playing an important pathophysiological role in the development of insulin resistance in type 2 DM patients [63]. NF- $\kappa$ B regulates various biological processes, including inflammation, apoptosis, and stress responses [7]. Elevated AGE/RAGE signaling in DM patients aggravates the NF- $\kappa$ B signaling and triggers the translocation of NF- $\kappa$ B into the nucleus, activating genes that produce pro-inflammatory cytokines, such as IL-1 $\beta$ , IL-6, IL-8, and MCP-1. Moreover, activation of NF- $\kappa$ B-dependent caspases regulate the apoptotic effects of TNF $\alpha$  [7]. The DM-associated corneal epithelial cells damage further triggers the release of inflammatory chemokines that stimulate the migration of resident DCs to the corneal wound bed, negatively influencing the DC-epithelial cell interaction and further exacerbating the pro-inflammatory environment [4]. Recently published research also demonstrated that 0.05 % fenofibrate instillation significantly reduced inflammatory cell infiltration and NF- $\kappa$ B expression in rat corneas following an alkali burn [20,24].

Our quantitative proteomic analysis in tears also identified several significantly altered proteins after fenofibrate treatment. IL1-RN is regarded as an antagonist of proinflammatory cytokines in the IL-1 family and regulates immune dysregulation [64,65]. The significantly elevated IL1-RN levels suggest the mechanism of action of fenofibrate in reducing ocular surface inflammation. The tear levels of pro-inflammatory C4B, CYB5A and CYB5B, on the other hand, were significantly reduced after treatment. C4B plays an important role in the complement activation, which subsequently regulates several stages of an inflammatory response [66]. Likewise, the accumulation of Cytochrome *b*<sub>558</sub> at the plasma membrane of phospholamban (PLB)-985 cells, a human diploid myeloid leukemia cell line, has been identified as

a marker of oxidative stress and related cell damage in phagocytic cells [67].

On the pathway analysis, those significantly dysregulated proteins were associated with several significantly expressed biological pathways, including the TCA cycle, oxidative phosphorylation, and LXR/RXR activation. The TCA cycle occurs in the mitochondria, and increasing evidence has suggested that stress conditions, such as DM, can damage intracellular mitochondria and release TCA cycle intermediates such as cytochrome *c* and ROS, resulting in cellular apoptosis [44]. Moreover, reduced ATP synthesis due to mitochondrial function dysregulation in DM patients may have a negative impact on ocular surface homeostasis, resulting in oxidative stress and an inflammatory tissue milieu. We also found that fenofibrate inhibited oxidative phosphorylation. During oxidative phosphorylation, oxidative stress occurs when there is an imbalance between mitochondrial ROS production and removal as a result of ROS overproduction and decreased antioxidant defense activity, which is more pronounced in DM patients [10]. Furthermore, fenofibrate reduces lipid levels by activating PPAR $\alpha$ , which forms a heterodimer with RXR [68]. The RXR/LXRs pathway regulates lipid and cholesterol metabolism [69]. Hypercholesterolaemia stimulates inflammatory responses, such as increased inflammasome activation, monocyte and neutrophil production [52]. Our data suggests that fenofibrate reduced ocular surface inflammation by regulating lipid metabolism and treating hyperlipidemia via LXR/RXR activation, hence lowering the inflammatory environment.

Corneal neuromas arise either following mechanical trauma to corneal nerves or in systemic diseases with aberrant nerve degeneration and regeneration, such as DM [70,71]. Our IVCN data showed that corneal neuromas were significantly more prevalent in DM patients than in healthy individuals, with significantly larger neuroma area, size, and perimeter. Fenofibrate treatment did not change the studied neuroma parameters, indicating that despite the anti-inflammatory effect, fenofibrate did not reverse the morphological damage on corneal nerves within the study period of 1 month. It implies that although corneal nerves can regenerate after fenofibrate treatment as we demonstrated previously [49,53], the nerve damage that generates corneal neuromas may not be reversed [72].

The current study has several limitations. Firstly, the changes in the age-matched control group were not examined, but limited changes in the parameters of interest in healthy adults are expected within 1-month period. Secondly, longer end point duration for fenofibrate treatment may be explored in future. Future research with a randomized controlled trial will be conducted to further validate the findings. Future studies will focus on topical fenofibrate formulations and comparable groups, such as topical cyclosporine or other anti-inflammatory drugs, as well as a variety of clinical scenarios involving ocular surface inflammation, such as chemical injury. Furthermore, topical fenofibrate formulations can eliminate the systemic side effects associated with oral fenofibrate intake, and the therapeutic benefit of topical fenofibrate on ocular surface inflammation will also be explored in the future. However, the aim of this study was to first establish the efficacy of oral fenofibrate in reducing ocular surface inflammation.

In conclusion, we demonstrated in this first clinical trial that oral fenofibrate reduced ocular surface inflammation by decreasing tear inflammatory cytokines while increasing anti-inflammatory mediators. It decreased corneal DC proliferation, increased CECD, improved TBUT and corneal integrity. Our study findings underscore the potential of oral fenofibrate as a treatment for diabetic ocular surface inflammation and its associated keratopathy. Given the high prevalence of diabetic ocular surface inflammation and the advantage of a shorter timeframe of repurposing an existing drug, fenofibrate could be a significant step towards mitigating the burden of diabetic ocular surface inflammation.

#### CRedit authorship contribution statement

**Hassan Mansoor:** Writing – review & editing, Writing – original



draft, Formal analysis. **Isabelle Xin Yu Lee:** Writing – review & editing, Investigation, Formal analysis. **Chang Liu:** Writing – review & editing, Investigation. **Mingyi Yu:** Writing – review & editing, Investigation. **Charmaine Jan Li Toh:** Writing – review & editing, Investigation, Formal analysis. **Victor Wei-Tsu Hsu:** Investigation, Formal analysis. **Fengyi Liu:** Investigation, Formal analysis. **Daqian Lu:** Investigation, Formal analysis. **Thomas Chuen Lam:** Investigation, Formal analysis. **Hong Chang Tan:** Writing – review & editing. **Lei Zhou:** Writing – review & editing, Investigation, Formal analysis. **Yu-Chi Liu:** Writing – review & editing, Supervision, Methodology, Funding acquisition, Formal analysis, Conceptualization.

## Disclosure

The authors have no conflict of interest.

## Funding

This work is supported by the Singapore National Medical Research Council grants MOH-CSAINV21jun-0001 and NMRC/OFLCG/001/2017, Clinician Scientist Individual Research Grant (CIRG24jul-0010).

## References

- [1] Tsalamandris S, Antonopoulos AS, Oikonomou E, Papamikroulis GA, Vogiatzi G, Papaioannou S, et al. The role of inflammation in diabetes: current concepts and future perspectives. *Eur Cardiol* 2019;14:50–9.
- [2] Mansoor H, Tan HC, Lin MT, Mehta JS, Liu YC. Diabetic corneal neuropathy. *J Clin Med* 2020;9.
- [3] So WZ, Qi Wong NS, Tan HC, Yu Lin MT, Yu Lee IX, Mehta JS, et al. Diabetic corneal neuropathy as a surrogate marker for diabetic peripheral neuropathy. *Neural Regen Res* 2022;17:2172–8.
- [4] Liu F, Liu C, Lee IXY, Lin MTY, Liu YC. Corneal dendritic cells in diabetes mellitus: a narrative review. *Front Endocrinol* 2023;14:1078660.
- [5] Priyadarsini S, Whelchel A, Nicholas S, Sharif R, Riaz K, Karamichos D. Diabetic keratopathy: insights and challenges. *Surv Ophthalmol* 2020;65:513–29.
- [6] Younessi P, Yoonessi A. Advanced glycation end-products and their receptor-mediated roles: inflammation and oxidative stress. *Iran J Med Sci* 2011;36:154–66.
- [7] Liu T, Zhang L, Joo D, Sun SC. NF-kappaB signaling in inflammation. *Signal Transduct Targeted Ther* 2017;2:17023.
- [8] Wan L, Bai X, Zhou Q, Chen C, Wang H, Liu T, et al. The advanced glycation end-products (AGEs)/ROS/NLRP3 inflammasome axis contributes to delayed diabetic corneal wound healing and nerve regeneration. *Int J Biol Sci* 2022;18:809–25.
- [9] Park JH, Kang SS, Kim JY, Tchah H. Nerve growth factor attenuates apoptosis and inflammation in the diabetic cornea. *Investig Ophthalmol Vis Sci* 2016;57:6767–75.
- [10] Buonfiglio F, Wasielica-Poslednik J, Pfeiffer N, Gericke A. Diabetic keratopathy: redox signaling pathways and therapeutic prospects. *Antioxidants* 2024;13.
- [11] Colorado LH, Beecher L, Pritchard N, Al Rashah K, Dehghani C, Russell A, et al. Corneal dendritic cell dynamics are associated with clinical factors in type 1 diabetes. *J Clin Med* 2022;11.
- [12] D'Onofrio L, Kalteniece A, Ferdousi M, Azmi S, Petropoulos IN, Ponirakis G, et al. Small nerve fiber damage and langerhans cells in type 1 and type 2 diabetes and LADA measured by corneal confocal microscopy. *Investig Ophthalmol Vis Sci* 2021;62:5.
- [13] Seifarth CC, Hinkmann C, Hahn EG, Lohmann T, Harsch IA. Reduced frequency of peripheral dendritic cells in type 2 diabetes. *Exp Clin Endocrinol Diabetes* 2008;116:162–6.
- [14] Vuckovic S, Withers G, Harris M, Khalil D, Gardiner D, Flesch I, et al. Decreased blood dendritic cell counts in type 1 diabetic children. *Clin Immunol* 2007;123:281–8.
- [15] Lagali NS, Badian RA, Liu X, Feldreich TR, Arnlov J, Utheim TP, et al. Dendritic cell maturation in the corneal epithelium with onset of type 2 diabetes is associated with tumor necrosis factor receptor superfamily member 9. *Sci Rep* 2018;8:14248.
- [16] Ge J, Jia Q, Liang C, Luo Y, Huang D, Sun A, et al. Advanced glycosylation end products might promote atherosclerosis through inducing the immune maturation of dendritic cells. *Arterioscler Thromb Vasc Biol* 2005;25:2157–63.
- [17] Bu Y, Shih KC, Kwok SS, Chan YK, Lo AC, Chan TCY, et al. Experimental modeling of cornea wound healing in diabetes: clinical applications and beyond. *BMJ Open Diabetes Res Care* 2019;7:e000779.
- [18] Gao N, Yin J, Yoon GS, Mi QS, Yu FS. Dendritic cell-epithelium interplay is a determinant factor for corneal epithelial wound repair. *Am J Pathol* 2011;179:2243–53.
- [19] Chow BJ, Lee IXY, Liu C, Liu YC. Potential therapeutic effects of peroxisome proliferator-activated receptors on corneal diseases. *Exp Biol Med* (Maywood) 2024;249:10142.
- [20] Arima T, Uchiyama M, Nakano Y, Nagasaka S, Kang D, Shimizu A, et al. Peroxisome proliferator-activated receptor alpha agonist suppresses neovascularization by reducing both vascular endothelial growth factor and angiopoietin-2 in corneal alkali burn. *Sci Rep* 2017;7:17763.
- [21] Uchiyama M, Shimizu A, Masuda Y, Nagasaka S, Fukuda Y, Takahashi H. An ophthalmic solution of a peroxisome proliferator-activated receptor gamma agonist prevents corneal inflammation in a rat alkali burn model. *Mol Vis* 2013;19:2135–50.
- [22] Nakano Y, Arima T, Tobita Y, Uchiyama M, Shimizu A, Takahashi H. Combination of peroxisome proliferator-activated receptor (PPAR) alpha and gamma agonists prevents corneal inflammation and neovascularization in a rat alkali burn model. *Int J Mol Sci* 2020;21.
- [23] Tobita Y, Arima T, Nakano Y, Uchiyama M, Shimizu A, Takahashi H. Peroxisome proliferator-activated receptor beta/delta agonist suppresses inflammation and promotes neovascularization. *Int J Mol Sci* 2020;21.
- [24] Nakano Y, Uchiyama M, Arima T, Nagasaka S, Igarashi T, Shimizu A, et al. PPARalpha agonist suppresses inflammation after corneal alkali burn by suppressing proinflammatory cytokines, MCP-1, and nuclear translocation of NF-kappaB. *Molecules (Basel)* 2018;24.
- [25] Tobita Y, Arima T, Nakano Y, Uchiyama M, Shimizu A, Takahashi H. Effects of selective peroxisome proliferator activated receptor agonists on corneal epithelial wound healing. *Pharmaceutics* 2021;14.
- [26] Jin L, Hua H, Ji Y, Jia Z, Peng M, Huang S. Anti-inflammatory role of fenofibrate in treating diseases. *Biomol Biomed* 2023;23:376–91.
- [27] Wright AD, Dodson PM. Medical management of diabetic retinopathy: fenofibrate and ACCORD Eye studies. *Eye (Lond)*. 2011;25:843–9.
- [28] Srinivas SP, Rao SK. Ocular surface staining: current concepts and techniques. *Indian J Ophthalmol* 2023;71:1080–9.
- [29] Miller KL, Walt JG, Mink DR, Satram-Hoang S, Wilson SE, Perry HD, et al. Minimal clinically important difference for the ocular surface disease index. *Arch Ophthalmol* 2010;128:94–101.
- [30] Teo CHY, Ong HS, Liu YC, Tong L. Meibomian gland dysfunction is the primary determinant of dry eye symptoms: analysis of 2346 patients. *Ocul Surf* 2020;18:604–12.
- [31] Pellegrini M, Bernabei F, Moscardelli F, Vagge A, Scotto R, Bovone C, et al. Assessment of corneal fluorescein staining in different dry eye subtypes using digital image analysis. *Transl Vis Sci Technol* 2019;8:34.
- [32] Chun YS, Yoon WB, Kim KG, Park IK. Objective assessment of corneal staining using digital image analysis. *Investig Ophthalmol Vis Sci* 2014;55:7896–903.
- [33] Chin JY, Tong L, Liu C, Lee IXY, Wong JHF, Wong RKT, et al. Quality of life and symptomatology in neuropathic corneal pain in comparison with dry eye syndrome. *Cornea* 2024.
- [34] Sall K, Foulks GN, Pucker AD, Ice KL, Zink RC, Magrath G. Validation of a modified national eye institute grading scale for corneal fluorescein staining. *Clin Ophthalmol* 2023;17:757–67.
- [35] Chin JY, Yang LWY, Ji AJS, Nubile M, Mastropasqua L, Allen JC, et al. Validation of the use of automated and manual quantitative analysis of corneal nerve plexus following refractive surgery. *Diagnostics* 2020;10.
- [36] Chin JY, Liu C, Lee IXY, Lin MTY, Cheng CY, Wong JHF, et al. Impact of age on the characteristics of corneal nerves and corneal epithelial cells in healthy adults. *Cornea* 2024;43:409–18.
- [37] Yawata N, Selva KJ, Liu YC, Tan KP, Lee AW, Siak J, et al. Dynamic change in natural killer cell type in the human ocular mucosa in situ as means of immune evasion by adenovirus infection. *Mucosal Immunol* 2016;9:159–70.
- [38] Chin JY, Lin MT, Lee IXY, Mehta JS, Liu YC. Tear neuromediator and corneal denervation following SMILE. *J Refract Surg* 2021;37:516–23.
- [39] Liu YC, Yam GH, Lin MT, Teo E, Koh SK, Deng L, et al. Comparison of tear proteomic and neuromediator profiles changes between small incision lenticule extraction (SMILE) and femtosecond laser-assisted in-situ keratomileusis (LASIK). *J Adv Res* 2021;29:67–81.
- [40] Yam GH, Fuest M, Zhou L, Liu YC, Deng L, Chan AS, et al. Differential epithelial and stromal protein profiles in cone and non-cone regions of keratoconus corneas. *Sci Rep* 2019;9:2965.
- [41] Jassal B, Matthews L, Viteri G, Gong C, Lorente P, Fabregat A, et al. The reactome pathway knowledgebase. *Nucleic Acids Res* 2020;48:D498–503.
- [42] Salinas RJMLO, Hernández RG, Crossa HJ. Generalized linear mixed models for non-normal responses. In: *Generalized linear mixed models with applications in agriculture and biology*. Cham: Springer; 2023. p. 113–27.
- [43] Choi I, Son H, Baek JH. Tricarboxylic acid (TCA) cycle intermediates: regulators of immune responses. *Life (Basel)* 2021;11.
- [44] White MJ, McArthur K, Metcalf D, Lane RM, Cambier JC, Herold MJ, et al. Apoptotic caspases suppress mtDNA-induced STING-mediated type 1 IFN production. *Cell* 2014;159:1549–62.
- [45] Zhao H, He Y, Ren YR, Chen BH. Corneal alteration and pathogenesis in diabetes mellitus. *Int J Ophthalmol* 2019;12:1939–50.
- [46] Weng J, Ross C, Baker J, Alfuraih S, Shamloo K, Sharma A. Diabetes-associated hyperglycemia causes rapid-onset ocular surface damage. *Investig Ophthalmol Vis Sci* 2023;64:11.
- [47] Naik K, Magdum R, Ahuja A, Kaul S, S J, Mishra A, et al. Ocular surface diseases in patients with diabetes. *Cureus* 2022;14:e23401.
- [48] Aggarwal S, Kheirkhah A, Cavalcanti BM, Cruzat A, Jamali A, Hamrah P. Correlation of corneal immune cell changes with clinical severity in dry eye disease: an in vivo confocal microscopy study. *Ocul Surf* 2021;19:183–9.
- [49] Mansoor H, Lee IXY, Lin MT, Ang HP, Xue YC, Krishna L, et al. Topical and oral peroxisome proliferator-activated receptor-alpha agonist ameliorates diabetic corneal neuropathy. *Sci Rep* 2024;14:13435.
- [50] Liang W, Huang L, Whelchel A, Yuan T, Ma X, Cheng R, et al. Peroxisome proliferator-activated receptor-alpha (PPARalpha) regulates wound healing and

- mitochondrial metabolism in the cornea. *Proc Natl Acad Sci USA* 2023;120: e2217576120.
- [51] Kaji Y, Usui T, Oshika T, Matsubara M, Yamashita H, Araie M, et al. Advanced glycation end products in diabetic corneas. *Investig Ophthalmol Vis Sci* 2000;41: 362–8.
- [52] Jiang QW, Kaili D, Freeman J, Lei CY, Geng BC, Tan T, et al. Diabetes inhibits corneal epithelial cell migration and tight junction formation in mice and human via increasing ROS and impairing Akt signaling. *Acta Pharmacol Sin* 2019;40: 1205–11.
- [53] Teo CHY, Lin MT, Lee IXY, Koh SK, Zhou L, Goh DS, et al. Oral peroxisome proliferator-activated receptor-alpha agonist enhances corneal nerve regeneration in patients with type 2 diabetes. *Diabetes* 2023;72:932–46.
- [54] Nakamura Y, Nakamura T, Tarui T, Inoue J, Kinoshita S. Functional role of PPARdelta in corneal epithelial wound healing. *Am J Pathol* 2012;180:583–98.
- [55] Avraham O, Feng R, Ewan EE, Rustenhoven J, Zhao G, Cavalli V. Profiling sensory neuron microenvironment after peripheral and central axon injury reveals key pathways for neural repair. *eLife* 2021;10.
- [56] Caillaud M, Patel NH, White A, Wood M, Contreras KM, Toma W, et al. Targeting Peroxisome Proliferator-Activated Receptor-alpha (PPAR- alpha) to reduce paclitaxel-induced peripheral neuropathy. *Brain Behav Immun* 2021;93:172–85.
- [57] Barathi VAWY, Luu CD, Wong TY, Chaurasia SS, Lamoureux EL. Effect of fenofibrate in hyperglycemic mice retina: role of downstream inflammatory cytokines in diabetic retinopathy. *Investig Ophthalmol Vis Sci* April 2014;55:1058.
- [58] Arango Duque G, Descoteaux A. Macrophage cytokines: involvement in immunity and infectious diseases. *Front Immunol* 2014;5:491.
- [59] Rath PC, Aggarwal BB. TNF-induced signaling in apoptosis. *J Clin Immunol* 1999; 19:350–64.
- [60] Choi KM, Lee J, Lee KW, Seo JA, Oh JH, Kim SG, et al. Comparison of serum concentrations of C-reactive protein, TNF-alpha, and interleukin 6 between elderly Korean women with normal and impaired glucose tolerance. *Diabetes Res Clin Pract* 2004;64:99–106.
- [61] Shikano M, Sobajima H, Yoshikawa H, Toba T, Kushimoto H, Katsumata H, et al. Usefulness of a highly sensitive urinary and serum IL-6 assay in patients with diabetic nephropathy. *Nephron* 2000;85:81–5.
- [62] Pickup JC, Chusney GD, Thomas SM, Burt D. Plasma interleukin-6, tumour necrosis factor alpha and blood cytokine production in type 2 diabetes. *Life Sci* 2000;67: 291–300.
- [63] Swaroop JJ, Rajarajeswari D, Naidu JN. Association of TNF-alpha with insulin resistance in type 2 diabetes mellitus. *Indian J Med Res* 2012;135:127–30.
- [64] Daull P, Barabino S, Feraille L, Kessal K, Docquier M, Parsadaniantz SM, et al. Modulation of inflammation-related genes in the cornea of a mouse model of dry eye upon treatment with cyclosporine eye drops. *Curr Eye Res* 2019;44:476–85.
- [65] Ortiz LA, Dutreil M, Fattman C, Pandey AC, Torres G, Go K, et al. Interleukin 1 receptor antagonist mediates the antiinflammatory and antifibrotic effect of mesenchymal stem cells during lung injury. *Proc Natl Acad Sci USA* 2007;104: 11002–7.
- [66] Markiewski MM, Lambris JD. The role of complement in inflammatory diseases from behind the scenes into the spotlight. *Am J Pathol* 2007;171:715–27.
- [67] Owusu SB, Dupre-Crochet S, Bizouarn T, Houee-Levin C, Baciou L. Accumulation of cytochrome b(558) at the plasma membrane: hallmark of oxidative stress in phagocytic cells. *Int J Mol Sci* 2022;23.
- [68] Deerochanawong C, Kim SG, Chang YC. Role of fenofibrate use in dyslipidemia and related comorbidities in the asian population: a narrative review. *Diabetes Metab J* 2024;48:184–95.
- [69] Schulman IG. Liver X receptors link lipid metabolism and inflammation. *FEBS Lett* 2017;591:2978–91.
- [70] Rosenthal P, Baran I, Jacobs DS. Corneal pain without stain: is it real? *Ocul Surf* 2009;7:28–40.
- [71] Sierra-Silvestre E, Andrade RJ, Colorado LH, Edwards K, Coppieters MW. Occurrence of corneal sub-epithelial microneuromas and axonal swelling in people with diabetes with and without (painful) diabetic neuropathy. *Diabetologia (Berl)* 2023;66:1719–34.
- [72] Toh CJL, Liu C, Lee IXY, Yu Lin MT, Tong L, Liu YC. Clinical associations of corneal neuromas with ocular surface diseases. *Neural Regen Res* 2024;19:140–7.